

# A Uniform Asymptotic Solution for Reflected and Scattered Fields over Half-Space Metamaterials

#Toru Kawano<sup>1</sup> and Toyohiko Ishihara<sup>2</sup>

<sup>1</sup>Department of Communication Engineering, National Defense Academy

<sup>2</sup>Retired from National Defense Academy

1-10-20 Hashirimizu, Yokosuka, Kanagawa 239-8686, Japan, tkawano@nda.ac.jp

## 1. Introduction

The problems of an electromagnetic wave that is incident on a plane dielectric interface consisting of two different mediums have been the important research subjects for many years [1] – [10]. When the beam is incident on the dielectric interface from the denser medium, the lateral displacement (or Goos-Hänchen shift) occurs at an angle that is slightly larger than the critical angle of the total reflection [1] – [4]. When the cylindrical wave is incident on the negative index material (NIM) from the positive index material (PIM) side, it has been shown that the backward lateral wave is excited along the interface between the NIM and the PIM [9].

In this work, we shall derive the novel uniform asymptotic solution for the reflected and scattered fields over half-space metamaterials with the negative refractive index [7] – [9]. The asymptotic solution consists of the geometrically reflected ray on the metamaterial, the backward lateral waves, and the transition wave which plays an important role in the transition region. The validity of the novel uniform asymptotic solution is confirmed by comparing with the reference solution calculated numerically from the integral representation.

## 2. Formulation and Uniform Asymptotic Solution

### 2.1 Formulation and Integral representation

Fig. 1 shows the schematic figure for the reflected and scattered fields over metamaterial, the two-dimensional coordinate system  $(x, z)$ , and the plane interface consisting of ordinary material and metamaterial. Medium 1 is ordinary material with the real permittivity  $\varepsilon_1$  and real permeability  $\mu_1$ , while medium 2 is metamaterial with complex permittivity  $\varepsilon_2$  and permeability  $\mu_2$ . The electric or the magnetic line source  $Q$  is located at  $(0, h)$  and the observation point  $P$  is located at  $(x, z)$  in the  $(x, z)$  two-dimensional coordinate system. At the observation point  $P(x, z)$ , the geometrically reflected ray  $Q \rightarrow A \rightarrow P$  reflected at the point  $A$  on metamaterial and the backward lateral wave are observed. Note that the backward lateral wave is excited by the incident geometrical ray  $Q \rightarrow B$  on metamaterial at the critical angle  $\hat{\delta}$  of the total reflection. The equiphase of the backward lateral

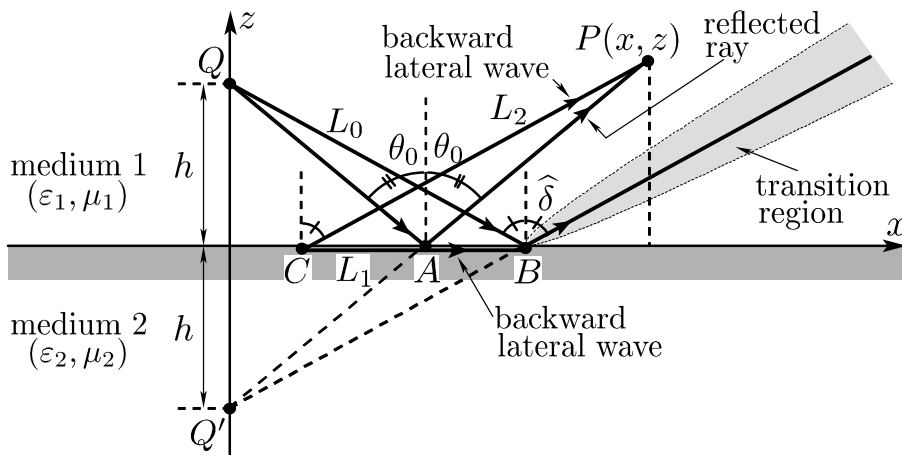


Figure 1: Schematic figure for reflected and scattered fields over half-space metamaterial and  $(x, z)$  two-dimensional coordinate system.  $\theta_0$ : incident angle of geometrically reflected ray,  $\hat{\delta}$ : critical angle of totally reflected ray.

wave propagates from  $C$  to  $B$  and from  $C$  to the observation point  $P$  as shown in Fig. 1.

These geometrically reflected ray and backward lateral wave solutions excited by the magnetic line source (H-type) may be obtained from the following integral [9]:

$$H_y^s = \frac{i}{4\pi} \int_{-\infty}^{\infty} \Gamma(k_{1x}) \frac{e^{ik_{1x} + ik_{1z}(z+h)}}{k_{1z}} dk_{1x}, \quad (1)$$

where  $k_{1x} (= \sqrt{k_1^2 - k_{1z}^2})$  and  $k_{1z}$  are respectively the  $x$ -component and the  $z$ -component of the free space wavenumber  $k_1$  in medium 1. The reflection coefficient  $\Gamma(k_{1x})$  may be given by [9]:

$$\Gamma(k_{1x}) = \frac{k_{1z}/\epsilon_1 - k_{2z}/\epsilon_2}{k_{1z}/\epsilon_1 + k_{2z}/\epsilon_2}, \quad k_{2z} = \sqrt{k_2^2 - k_{1x}^2}, \quad k_{1x} = k_{2x}, \quad (2)$$

where  $k_2 (= \omega\sqrt{\epsilon_2\mu_2})$  is the free space wavenumber in metamaterial (medium 2) and  $k_{2x}$  denotes the  $x$ -component of  $k_2$ . The scattered magnetic field  $H_y^s$  in (1) directing the perpendicular direction to the paper (or the  $y$ -direction) in Fig. 1 may be transformed to the complex  $\theta$ -plane via  $k_{1x} = k_1 \sin \theta$ . The integral in the complex  $\theta$ -plane may be given by

$$H_y^s = \frac{i}{4\pi} \int_{P_\theta} \Gamma(k_1 \sin \theta) e^{ik_1 R_1 q(\theta)} d\theta, \quad (3)$$

$$\Gamma(k_1 \sin \theta) \equiv \Gamma(\theta) = \frac{m \cos \theta - \sqrt{n^2 - \sin^2 \theta}}{m \cos \theta + \sqrt{n^2 - \sin^2 \theta}}, \quad (4)$$

$$q(\theta) = \cos(\theta - \theta_0), \quad (5)$$

where the propagation distance  $R_1$  and the incident angle  $\theta_0$  of the reflected ray  $Q \rightarrow A \rightarrow P$  used in the above equations are defined geometrically in Fig. 1 and  $m$  and  $n$  in (4) are defined as follows:

$$m = \frac{\epsilon_2}{\epsilon_1}, \quad n = \frac{\sqrt{\epsilon_2\mu_2}}{\sqrt{\epsilon_1\mu_1}}. \quad (6)$$

The integration contour  $P_\theta$  and the branch points at  $\theta = \pm\hat{\delta}$  associated with the branch cuts ( $\hat{\delta}$  and  $-\hat{\delta}$ ) of the integrand in (3) are shown in Fig. 2 in the complex  $\theta$ -plane. The branch point  $\theta = \hat{\delta}$  is defined by  $\hat{\delta} = \sin^{-1} \hat{n}$ ,  $\hat{n} = -n$ . In the following section, we shall derive the uniform asymptotic solution from (3) by applying the high-frequency saddle point technique.

## 2.2 Uniform Asymptotic Solution for Reflected and Scattered Fields

When the high-frequency condition  $k_1 R_1 \gg 1$  is satisfied, the integrand in (3) possesses the saddle point at  $\theta = \theta_0$  determined from  $(\partial/\partial\theta)q(\theta) = 0$  (see (5)). Thus the integral in (3) may be evaluated by applying the saddle point technique after deforming the original integration path  $P_\theta$

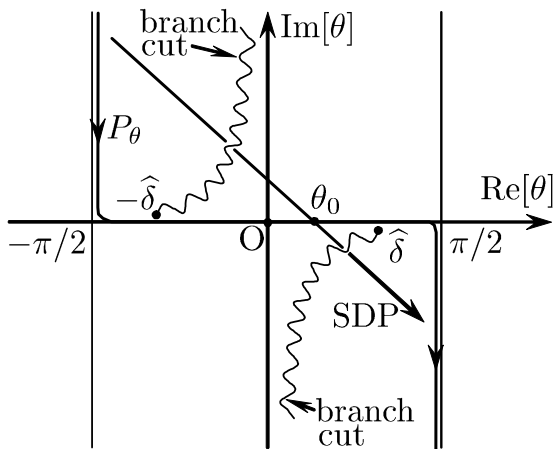


Figure 2: The original integration contour  $P_\theta$ , the branch points  $\pm\hat{\delta}$  associated with the branch cuts, and the steepest descent path (SDP).

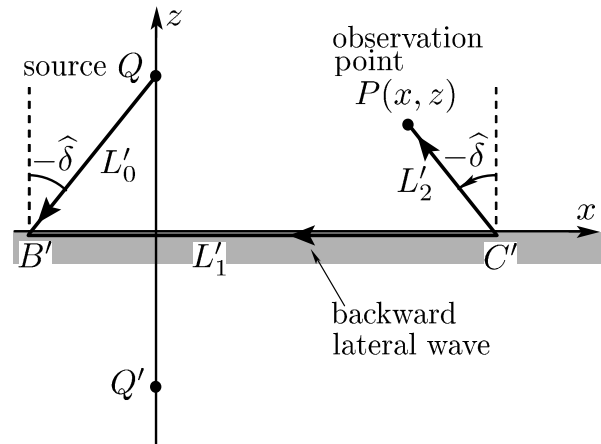


Figure 3: Second kind of backward lateral wave excited by the geometrical ray  $Q \rightarrow B'$  incident on the point  $B'$  at the critical angle  $-\hat{\delta}$ .

into the steepest descent path (SDP) passing through the saddle point  $\theta = \theta_0$  (see Fig. 2). As shown in Fig. 2, the branch cut (or cuts) is (or are) traversed by the steepest descent path (SDP). Thus the contributions to the integral in (3) may arise from the integration along the SDP and from the integration around the branch cut (or cuts) [6], [10]. The novel uniform asymptotic solution may be represented by [6], [10]:

$$H_y^s = H_y^{go} + U(\hat{\delta} - \theta_0)H_y(\hat{\delta}) + H_y(-\hat{\delta}) + H_y^{tran}, \quad (7)$$

where  $H_y^{go}$  denotes the geometrically reflected ray  $Q \rightarrow A \rightarrow P$  (see Fig. 1).  $H_y(\hat{\delta})$  is the contribution from the integration around the branch point  $\theta = \hat{\delta}$  and denotes the backward lateral wave shown in Fig. 1. The notation  $U(\hat{\delta} - \theta_0)$  denotes the unit step function where  $U(\hat{\delta} - \theta_0) = 1$  for  $\hat{\delta} > \theta_0$  and  $U(\hat{\delta} - \theta_0) = 0$  for  $\hat{\delta} < \theta_0$ . Thus the backward lateral wave  $H_y(\hat{\delta})$  can be observed in the region satisfying  $\hat{\delta} > \theta_0$  (see Fig. 1). While,  $H_y(-\hat{\delta})$  in (7) arises from the integration around the branch point at  $\theta = -\hat{\delta}$  and denotes the second kind of the backward lateral wave shown in Fig. 3. The last term  $H_y^{tran}$  defined as the ‘‘transition wave’’ plays an important role only in the transition region near the critical angle  $\hat{\delta}$  (i.e.,  $\theta_0 \approx \hat{\delta}$ ) shown in Fig. 1. We assume that the observation point is placed at  $P(x, z)$  where  $x, z > 0$ . Then the asymptotic solutions may be given by

$$H_y^{go} = \frac{i}{4} \sqrt{\frac{2}{\pi k_1 R_1}} e^{ik_1 R_1 - i\pi/4} \Gamma(\theta_0), \quad (8)$$

$$H_y(\hat{\delta}) = \frac{\exp(i\pi/4)\sqrt{\hat{n}}}{\sqrt{2\pi \hat{m} k_1^{3/2} (1 - \hat{n}^2) L_1^{3/2}}} e^{ik_1(L_0 + L_2) - ik_2 L_1} \frac{D_{-3/2}(\xi + i\xi)}{2^{-3/4} \xi^{-3/2} \exp(-i3\pi/8) \exp(-i\xi^2/2)}, \quad (9)$$

$$\xi = \sqrt{2k_1 R_1} \sin \frac{\hat{\delta} - \theta_0}{2}, \quad \hat{n} = -n, \quad \hat{m} = -m, \quad \hat{k}_2 = -k_2, \quad (10)$$

$$H_y(-\hat{\delta}) = \frac{\exp(i\pi/4)\sqrt{\hat{n}}}{\sqrt{2\pi \hat{m} k_1^{3/2} (1 - \hat{n}^2) L_1'^{3/2}}} e^{ik_1(L_0' + L_2') - ik_2 L_1'}, \quad (11)$$

$$H_y^{tran} = \Gamma^{(2)}(\hat{\delta}) \sqrt{\sin(\hat{\delta} - \theta_0)} \frac{i}{4} \sqrt{\frac{2}{\pi k_1 R_1}} e^{ik_1 R_1 - i\pi/4} \left\{ \frac{D_{1/2}(|\xi| - i|\xi|)}{2^{1/4} |\xi|^{1/4} e^{-i\pi/8} e^{i\xi^2/2}} - 1 \right\}, \quad (12)$$

$$\Gamma^{(2)}(\hat{\delta}) = -\frac{2\sqrt{2\hat{n}}}{\hat{m}\sqrt{\cos \hat{\delta}}}, \quad (12a)$$

where  $D_{-3/2}(\cdot)$  and  $D_{1/2}(\cdot)$  are the parabolic cylinder functions [10], [11] and the notations  $L_0, L_1, L_2$ , used in the above equations are defined geometrically in Fig. 1 while  $L_0', L_1', L_2'$ , are defined

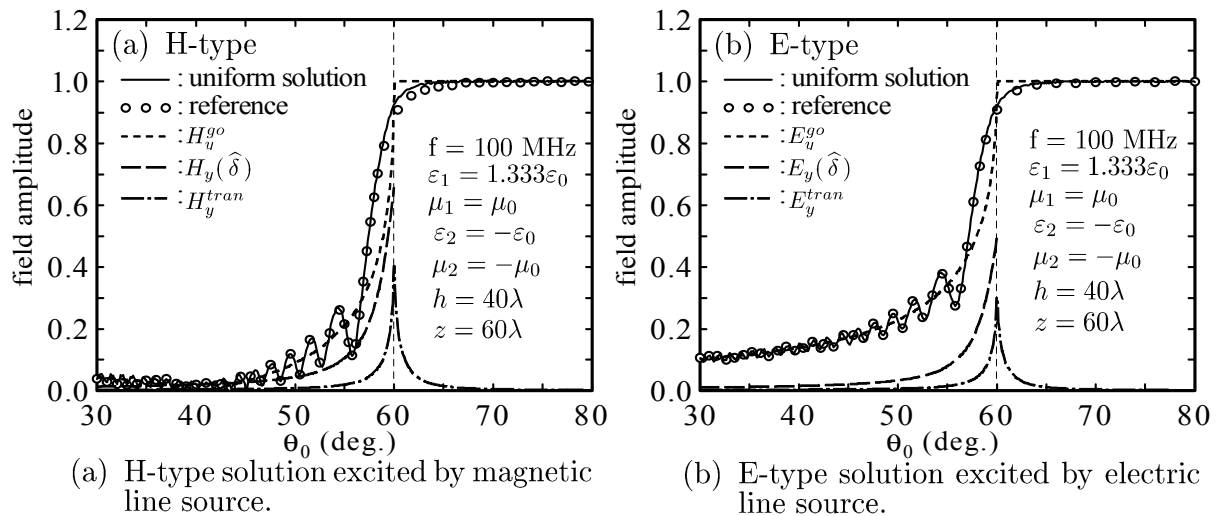


Figure 4: Comparisons between the uniform asymptotic solution in (7) and the reference solution calculated numerically from the integral in (3).

geometrically in Fig. 3.

When the observation point  $P$  is located far away from the transition region,  $|\xi|$  defined in (10) takes the large values i.e.,  $|\xi| \gg 1$ . Then the parabolic cylinder function  $D_{1/2}(\xi - i|\xi|)$  [10], [11] is approximated by

$$D_{1/2}(x - ix) \approx 2^{1/4} x^{1/2} e^{-i\pi/8} e^{ix^2/2}. \quad (13)$$

Therefore the terms inside the parentheses  $\{ \}$  in (12) approach zero as the value of  $|\xi|$  increases. This is the reason why  $H_y^{tran}$  in (12) is defined as the “transition wave”. The transition wave plays an important role only in the transition region.

### 3. Numerical Results and Discussions

In Fig. 4(a), we have calculated the reflected and scattered magnetic fields  $H_y^s$  by using the novel uniform asymptotic solution derived in (7) associated with (8) – (12a) and compared with the reference solution calculated from the integral in (3) by applying the numerical integration along the original integration contour  $P_\theta$ . We have also calculated  $H_y^{go}$ ,  $H_y(\hat{\delta})$ , and  $H_y^{tran}$  separately which compose the uniform asymptotic solution in (7). Note that the second kind of the backward lateral wave  $H_y(-\hat{\delta})$  in (7) is negligibly small compared with other terms (see Fig. 3). It is shown that the uniform asymptotic solution (— : solid curve) agrees very well with the reference solution (ooo : open circles). One may observe that, as the observation point moves toward the backward direction, the backward lateral wave (— —) decays algebraically according to  $1/L_1^{3/2}$  (see (9) and Fig. 1). One may also observe that the transition wave (— · —) plays an important role only in the transition region near the critical angle  $\hat{\delta} \approx 60^\circ$ .

Fig. 4(b) shows the E-type scattered field excited by the electric line source  $Q$  (see Fig. 1). It is clarified that the E-type uniform asymptotic solution agrees excellently with the reference solution.

### 4. Conclusion

We have derived the novel uniform asymptotic solution for the reflected and scattered fields over half-space metamaterial. The uniform asymptotic solution consists of the geometrically reflected ray, the backward lateral waves, and the transition wave which plays an important role only in the transition region near the critical angle. The validity of the uniform asymptotic solution is confirmed by comparing with the reference solution calculated numerically.

### References

- [1] H. K. V. Lotsch, OPTIK, vol.32, no.2, pp.116-137, April 1970.
- [2] B. R. Horowitz and T. Tamir, J. Opt. Soc. Am., vol.61, pp.586-594, May 1971.
- [3] B. R. Horowitz and T. Tamir, Appl. Phys. vol.1, pp.31-38, 1973.
- [4] J. W. Ra, H. L. Bertoni, and L. B. Felsen, SIAM. Math. vol.24, no.3, pp.396-413, May 1973.
- [5] S. Kozaki, and H. Sakurai, J. Opt. Soc. Am., vol.68, no.4, pp.508-514 April 1978.
- [6] T. Ishihara and Y. Miyagawa, Trans. on IEICE, vol.J82-C-1, no.2, pp.62-73, Feb. 1999.
- [7] P. M. Valanju, R. M. Walser, and A. P. Valanju, Physical Review Letters, vol.88, no.18, pp.187401-1-187401-4, May 2002.
- [8] D. R. Smith, D. Schurig, and J. B. Pendry, Applied Physics Letters, vol.81, no.15, pp.2713-2715, Oct. 2002.
- [9] A. Ishimaru and J. R. Thomas, IEEE Trans. on Antennas & Propag., vol.53, no.3 p.915-921, March 2005.
- [10] H. Yamada, T. Kawano, K. Goto, and T. Ishihara, Proc. of the International Symposium on Antennas and Propagation (ISAP), pp.181-184, CD-ROM (ISBN 978-4-88552-223-9 (3055©IEICE) Niigata, Japan, August 2007.
- [11] E. T. Whittaker and G. N. Watson, eds., A Course of Modern Analysis, pp.347-351, Cambridge University Press, Cambridge, 1973.